Journal of Physics and Chemistry of Solids 106 (2017) 58–64

Contents lists available at ScienceDirect

Journal of Physics and Chemistry of Solids

journal homepage: www.elsevier.com/locate/jpcs

Synthesis, X-ray crystal structure and highly non-linear optical properties of inorganic-organic hybrid compound: 1,4-Diazbicyclo-octane oxonium tri-nitrates single crystal

Rokaya Henchiri[a,b], Nasreddine Ennaceur[a,b,*], Marie Cordier[c], Isabelle Ledoux-Rak[b], Elimame Elaloui[a]

[a] Laboratory of Materials, Energy and Environment UR14-ES26, University of Gafsa, 2100 Gafsa, Tunisia
[b] Laboratory of Quantum and Molecular Photonics, Institut d'Alembert, Ecole Normale Supérieure de Cachan, 94230 Cachan, France
[c] Molecular Chemistry Laboratory, UMR 9168, Ecole Polytechnique, CNRS, 91128 Palaiseau Cedex, France

ARTICLE INFO

Keywords:
Crystal structure
X-ray diffraction
Optical materials
High nonlinearity
Infrared spectroscopy
Thermal behavior

ABSTRACT

A new nonlinear optical hybrid crystal 1,4-Diazbicyclo[222]octane oxonium tri-nitrates (DOTN), of the dimension 4×12×1 mm^3. The crystal was grown using water as solvent at room temperature and crystal structure was determined by X-Ray diffraction respectively, this title compound was shown to crystallize in non-centrosymmetric trigonal system with space group P31c. The recorded FTIR spectrum has proven the presence of various functional groups in the grown crystal as well as the formation of DOTN. Besides, the thermal stability and melting temperature of the DOTN crystal were identified from the TG/DSC analysis. The suitability of this material for optical application was studied by non-linear optical (NLO) and UV–visible absorption techniques. Furthermore, the nonlinear optical property was analyzed by Kurtz-Perry powder technique and was 3.4 times than that of KDP (potassium dihydrogen phosphate) single crystals. The first hyperpolarizability of nitrate was determined by Second Harmonic light Scattering.

1. Introduction

Nonlinear optics has been given increasing attention due to its wide application in electronics, data storage technology and optical communication [1]. These applications require the presence of extraordinary physical properties, such as NLO which is the key element for future technologies in physical optics [2]. Firstly, the research works have concentrated on inorganic materials such as KDP, lithium niobate ($LiNbO_3$) and its analogues [3]. However, inorganic crystals face a 'trade-off' problem between the amplitude of the optical nonlinearity and response time [4–7]. Recently, organic materials with delocalized conjugated π-electrons have gained much attention due to their large NLO properties and good response. Although these materials have the capacity to double the frequency of incident light and have important commercial applications due to high second-order nonlinear coefficients, their transparency domain has been reduced. Likewise, they suffer from problems such as low thermal stability, mechanical weakness, etc. [8–11].

Presently, inorganic and organic materials are being swapped by hybrid compounds. The latter, share the properties of both inorganic and organic materials. Recent interest has been focused on the metal complexes of organic compounds due to their large non-linearity [12]. The approach of combining the high nonlinear optical coefficients of the organic molecules with the good physical properties of the inorganic ones has been very successful, in recent years. Hence, current research is interested in semi-organic materials due to their exceptional nonlinearity, high resistance to laser induced damage and good mechanical stability [13]. Actually, the amines, mineral acids and salts have also been proven to be attractive materials in optoelectronic applications as they contain a proton-donating acid group and proton-accepting amino group [14]. The amino acids and inorganic acids complexes are promising materials for the optical second harmonic generation (SHG), as they tend to combine the benefits of the organic amino acid and the inorganic acid [15].

Heteroaromatic derivatives are a group of organic compounds that have demonstrated their unique properties in the field of the non linear optics because of the delocalized cloud of π electrons [16–18]. 1,4-diazabicyclo[2.2.2]octane (dabco) is a nucleophilic amine commonly used in the catalytic field [19,20] and it is a very useful organic molecule in building phase transition crystals because of its extremely

* Corresponding author at: Laboratory of Materials, Energy and Environment UR14-ES26, University of Gafsa, 2100 Gafsa, Tunisia.
E-mail address: nasr.ennaceur@yahoo.fr (N. Ennaceur).

http://dx.doi.org/10.1016/j.jpcs.2017.02.011
Received 21 November 2016; Received in revised form 15 February 2017; Accepted 19 February 2017
Available online 09 March 2017

symmetric form that tends to pursue order-disorder transformations in crystals and its multiple roles in formation of hydrogen bonds by acting either H donor or acceptor or both [21–25].

In this paper, we have reported the studies of the synthesis, crystal structure and physical properties of DOTN which is a hybrid crystal with excellent nonlinear coefficient. The crystal was grown using water as solvent at room temperature and crystal structure was determined by X-Ray diffraction respectively. It was found to be of a non-centrosymmetric space group P31c, which is required for the physical property. The optical and thermal stability as well as the second harmonic generation properties of DOTN were also reported in this research work.

2. Experimental details

2.1. Growth of DOTN single crystals

The low temperature solution growth technique was used for the growth of DOTN which is widely used for the growth of inorganic and organic single crystals to get more transparent single crystals. The starting compounds, namely,1,4-diazabicyclo[2.2.2]octane (Sigma Aldrich, 99%) and nitric acid (Sigma Aldrich, 96%) were used without further purification. The single crystals of DOTN were successfully grown from slow evaporation solution growth technique at room temperature in the non-stoichiometric ratio, with deionized water as solvent. The saturated solution of DOTN was obtained by dissolving the charge material into the purified water with continuous stirring of the solution using an immersible magnetic stirrer at room temperature. DOTN was synthesized according to the following chemical reaction.

$$C_6H_{12}N_2 + 3\ HNO_3 \xrightarrow{H_2O} C_6H_{14}N_2.\ (NO_3)_3.\ H_3O^+$$

After 15 days of growth, the colorless single crystal of the dimension of 12×9×4 mm^3 was obtained by slow evaporation technique. The photograph of the as grown crystal of DOTN is shown in Fig. 1. The crystal had good compositional stability and showed no degradation when keep in the open air for several months.

2.2. Single crystal X-ray diffraction

The single crystal of DOTN compound was mounted on a Kapton loop using a Paratone N oil. An APEX II CCD BRUKER detector and a graphite Mo-Kα monochromator was used to obtain the data. All measurements were taken at 150 K and a refinement method was used for solving the structure. The structure resolution was accomplished using the SHELXT-2014 [26] program and the refinement was done with the SHELXL-2014 program [27]. The structure solution and the refinement were achieved with the PLATON software. During the refinement steps, all atoms- except hydrogens- were refined anisotropically. The position of the hydrogens was determined using residual electronic densities, which are calculated by a Fourier difference. The XRD study has revealed that the single crystal belongs to trigonal system, with a space group of P31c with the lattice parameters a=10.0304(5) Å, b=10.0304(5) Å, c=7.1558(5) Å and V=623.48(8) $Å^3$. The crystal data and structure refinement of the DOTN material are given in Table 1. The fractional atomic coordinates and isotropic or equivalent isotropic displacement parameters are summarized in Table 2. For further details of the structure identification, they are available from the Cambridge crystallographic data centre (CSD) CCDC 1406643.

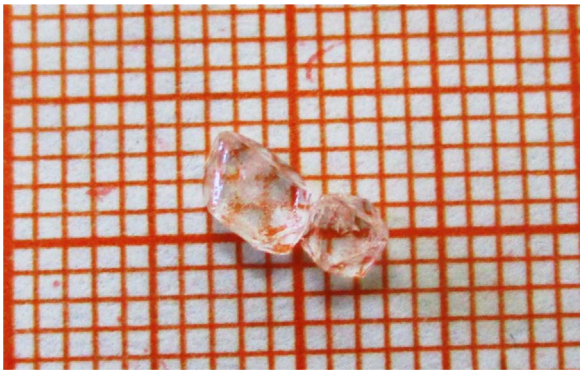

Fig. 1. Photograph of as-grown DOTN crystal.

Table 1
The crystal data and the structure refinement of DOTN material.

Crystal data	
Chemical formula	$C_6H_{14}N_2\ (NO_3)_3.H_3O$
Formula weight (g mol^{-1})	319.24
Crystal system	Trigonal
Space group	P 3 1 c
a (Å)	10.0304 (5)
	7.1558 (5)
b (Å)	10.0304 (5)
c (Å)	7.1558 (5)
F(000)	336
V ($Å^3$)	623.48
Z	2
Crystal size (mm^3)	0.400×0.120×0.100
Color	Colorless
Intensity data collection	
Diffractometer	Kappa Apex II
Wavelength	λ (Kα)=0.71069 Å
Absorption corrections	Multi-scan
Temperature (K)	150
θ range for data collection (deg)	1.9≤θ≤30.009
Range of *h*, *k*, *l*	−14≤h≤8; −10≤k≤9; −10≤1≤7
Reflections measured	2375
Independent reflections [I > 2σ (I)]	968
Structure refinement	
Computer programs	ShelxT et Shelxl
Refinement	based of F^2
Electron density residuals (e. $Å^{-3}$)	−0.19 < Δρ < 0.24
Goodness-of-fit on F^2	1.004
Flack parameter	0.00 (1)
wR_2 (%)	8.68
R_1 (%)	3.55
Cambridge Crystallographic Data Centre (CSD)	CCDC 1406643

Table 2
Fractional atomic coordinates and isotropic or equivalent isotropic displacement parameters ($Å^2$).

	x	*y*	*z*	U_{iso}*/U_{eq}
N1	0.3460 (2)	0.2167 (2)	0.2672 (3)	0.0166 (4)
N2	0.3333	0.6667	0.4167 (5)	0.0140 (6)
H2	0.3333	0.6667	0.538 (9)	0.017*
N3	0.3333	0.6667	0.0683 (5)	0.0146 (6)
H3	0.3333	0.6667	−0.060 (9)	0.018*
C1	0.1804 (3)	0.5404 (3)	0.3484 (4)	0.0163 (4)
H1A	0.161 (4)	0.452 (4)	0.417 (5)	0.020*
H1B	0.104 (4)	0.572 (3)	0.373 (5)	0.020*
C2	0.1970 (3)	0.5208 (3)	0.1389 (4)	0.0176 (4)
H2A	0.110 (4)	0.508 (4)	0.074 (5)	0.021*
H2B	0.213 (4)	0.437 (3)	0.112 (5)	0.021*
O1	0.2542 (2)	0.2464 (2)	0.3550 (3)	0.0268 (5)
O2	0.3027 (2)	0.0835 (2)	0.2150 (3)	0.0268 (5)
O3	0.48106 (18)	0.3242 (2)	0.2387 (3)	0.0207 (4)
O4	0.0000	0.0000	0.4353 (5)	0.0212 (7)
H4	−0.005 (6)	−0.094 (6)	0.392 (8)	0.070 (16)*

* Corresponding to the hydrogen atoms (H) mentioned in the table which are refined isotrpically.

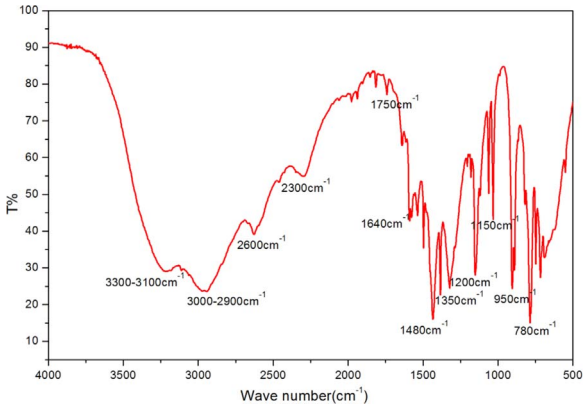

Fig. 2. FTIR spectrum of DOTN crystal.

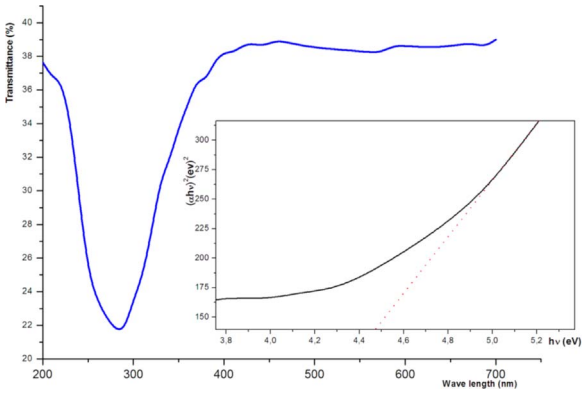

Fig. 3. UV–vis absorption spectrum.

2.3. FT-IR studies

The FT-IR studies were carried out with freshly crushed samples mixed with KBr and palletized using a hydraulic press. The spectra were recorded in the range of 500–4000 cm^{-1} using the BRUKER IFS–66V spectrometer. Fig. 2 shows FTIR spectrum of the grown DOTN crystal.

The peak appearing at 3152 cm^{-1} is due to O–H vibration, which indicates the presence of oxonium in the crystal lattice. Furthermore, the peaks appear at 2782 cm^{-1} and 1571 cm^{-1}, indicating the symmetric and bending vibrations of NH^{+}. The peaks appearing at 2890 cm^{-1} and 1427 cm^{-1} are due to the symmetric and bending C–H stretching frequency. The asymmetric and symmetric stretching frequency for NO_3^- ion is observed at 1650 cm^{-1} and 1461 cm^{-1}. The peak detected at 1228 cm^{-1} is assigned to the symmetric stretching frequency of C–N group vibrations. Table 3 shows the frequency assignment of DOTN crystal.

2.4. UV–vis spectral analysis

The UV transmission spectra are very significant for any optical material since a nonlinear optical material is of a practical use only if it has an extensive transparency window. Indeed, UV–vis studies provide important information about the structure of DOTN because the absorption of UV and visible light involves the promotion of the electrons in σ and π orbitals from the ground state to higher energy states. Within this framework, the UV–vis transmission spectrum is studied by Perkin Elmer lambda 35 UV–vis spectrophotometer. Cut and polished crystal with 1 mm thickness was used for UV–vis studies. Fig. 3 shows the optical transmission spectrum of the DOTN crystal. The crystal shows good transmittance of more than 37% in the visible region. This huge transparence makes the crystal suitable for nonlinear applications. This is an advantage of the use of amines, where the absence of strongly conjugated bonds leads to wide transparency ranges in the visible and UV spectral regions. The lower cut-off wavelength of DOTN crystal is at 280 nm and therefore wide transmission window exists in visible region, which plays very useful role in nonlinear application of optical material. Optical band gap (Eg) value was calculated from the graph of $(\alpha h\upsilon)^2$ vs $h\upsilon$ [28], where α is the absorption coefficient and E = hυ is the energy of the photon. The band gap was estimated as 4.47 eV by extrapolating the linear portion near the onset of transmission edge to the energy axis (Fig. 3). The absence of absorption bands in the visible region and the wide band gap of the grown crystal are incredibly suitable for photonic and optical applications [29].

Table 3
Assignment of IR band frequencies (cm^{-1}) observed for DOTN.

Band frequencies for DOTN (cm^{-1})	Assignment
917	O–H out of plane bending
1228	C–N symmetric stretching
1400	O–H in plane bending
1427	C–H stretching
1461	NO_3^- symmetric stretching
1571	N^+–H bending of NH_2
1650	NO_3^- asymmetric stretching
2782	N^+–H symmetric stretching
2980	C–H symmetric stretching
3152	O–H symmetric stretching

2.5. Thermal analysis

Generally, thermal analysis gives information about dehydration, enthalpy, mass change, melting, decomposition, phase analysis etc. The TG/DSC of DOTN has been recorded by using PerkinElmer Diamond TG/DSC instrument. A platinum crucible was used to heat the sample. This thermal analysis was conducted in an atmosphere of nitrogen at a heating rate of 10 °C/min in the temperature range of 40–400 °C. The initial mass of the analyzed material subjected to the analysis was 9 mg. The TG/DSC is shown in Fig. 4. TG curve revealed that there are two-steps weight losses. The first decomposition, from 87 to 115 °C, is due to the loss of the Hydronium molecule (experimental weight loss: 7.3% and theoretical weight loss: 5.95%). The second stage which starts at about 155 °C and ends above 178 °C, is assigned to the destruction of the organic entities (experimental loss: 39% and theoretical loss: 35.37%) and the volatilization of the compound. This phenomenon is accompanied by two sharp endothermic and exothermic peaks observed on the DSC curve at about 113 and 173 °C, respectively.

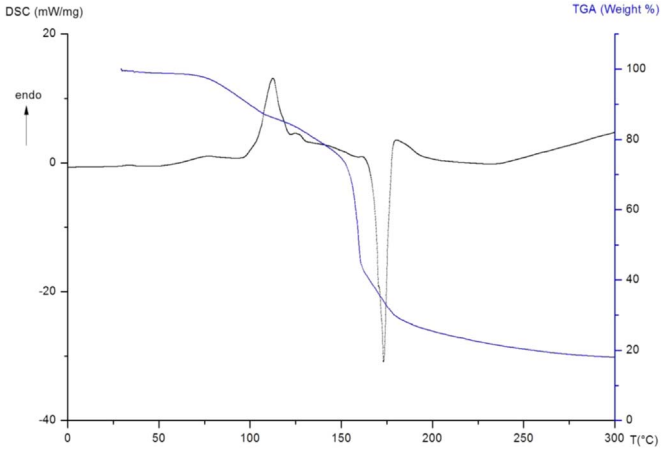

Fig. 4. TGA and DSC thermograms of the DOTN crystal.

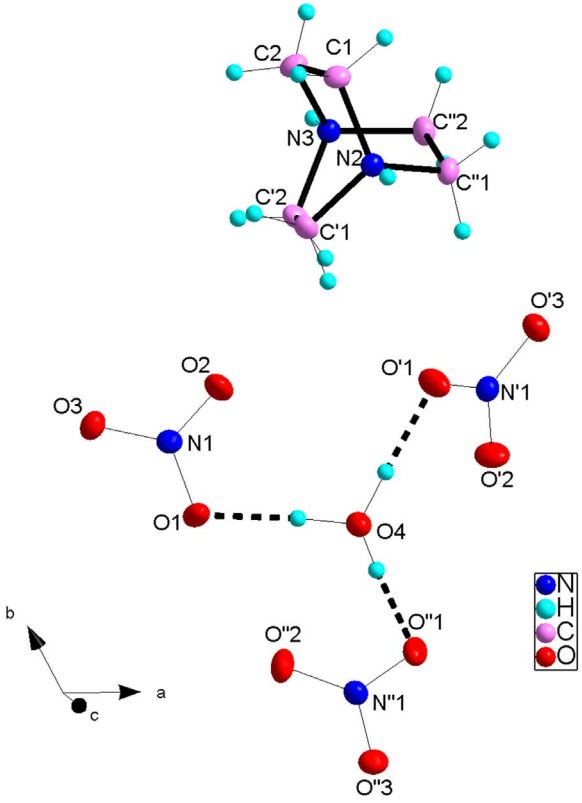

Fig. 5. The asymmetric unit of the DOTN compound.

3. Results and discussion

3.1. Description of the structure

The structural determination of DOTN compound has established the structural model in which the asymmetric unit (Fig. 5) consists of an organic cation $(C_6H_{14}N_2)^{2+}$ diprotonated, three inorganic anions NO_3^- and H_3O^+ molecule. These entities are linked by hydrogen bonds and π-π interactions involving a crystal structure in a three-dimensional network. Fig. 6 shows the projection of the crystal structure of DOTN in the (a, b) plane. The anionic group composed of nitrates developed in wire along the [001] direction alternately with the cationic group consisting of organic cations $(C_6H_{14}N_2)^{2+}$ and hydronium ions H_3O^+. The latter are inserted between the organic (cationic) and mineral (anionic) groups, which provide stability and cohesion of the structure.

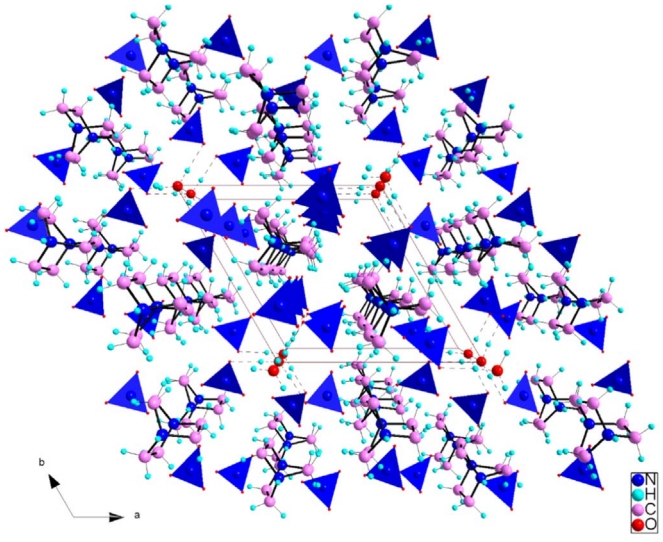

Fig. 6. The projection of the crystal structure of DOTN in the (a, b) plane.

3.1.1. The cationic group

The cationic part is consisted of two molecules, DABCO ($(C_6H_{14}N_2)^{2+}$) and hydronium (H_3O^+): In the asymmetric unit, $^1/_3$ of the molecule of DABCO was observed, and the remaining $^2/_3$ were generated by a 3-fold axis with symmetry (−x+y, −x+1, and z -y+1, x-y +1, z). These organic cations interposed between the channels of nitrates develop in zigzag and parallel to the (a, c) plane with the mean axis a=0 (Fig. 6). The N-C distances are equal to 1.505 (3) and 1.501 (3) Å. There are alternating short and long links, which may be due to the electron delocalization of a π-conjugated system. The values of the average distances of C-C and C-H are equal to 1.532 and 0.95 Å, respectively. Similarly, the angle C-N-C and N-C-C are successively around 109 and 107°. The distances and angles in the DABCO cycle are similar to those encountered in other studied structures [30]. The hydronium environment consists of three nitrate molecules that are bound by C_3 symmetry. The interaction among these molecules is provided by several hydrogen bonds.

3.1.2. The anionic group

In the nitrate anion NO_3^-, the N-O distances and O-N-O angles accord well with the already-described structures in the reviewed literature [15]. It is clearly seen that the nitrate anions are developed along the a-axis in two altered levels: zigzagging with a mean b-axis =3/4 and regular with b=1/3 (Fig. 6). The detailed geometry of the nitrate entities shows that the N1–O2 [1.2381(0) Å] and N1–O3 bond [1.2565(1) Å], bond lengths are significantly shorter than the N1–O1 [1.2671(0) Å], which is in accordance with the relatively strong interaction involving the O1 atom with the hydronium molecule O4–H4···O1 [2.576 (2) Å]. On the other hand, the nitrate group acts as a hydrogen-bond acceptor from five neighboring DABCO cations through a weak C–H···O and N–H···O interactions, and therefore ensures the anion–cation connection along the a- and c-axes.

3.1.3. The hydrogen bonds

The structure of the solid solution $C_6H_{14}N_2,(NO_3)_3{\cdot}H_3O$ is stabilized by different intermolecular hydrogen bonds (strong and weak) and electrostatic interactions of Van der Waals. Fig. 7 and Table 4 show the three oxygen atoms O_1, O_2 and O_3 of the nitrate ion that are involved in several interactions (O···N, O···C and O···O) with organic cations and hydronium H_3O^+ ion. All these bonds are generated by C_3 symmetry. Indeed, the interactions DABCO-NO_3^- are firstly weak hydrogen bonds N_2-H_2···O_3=2.935(3) and N_3-H_3···O_3=2.978(3) Å, and secondly weak C–H···O intermolecular interactions whose donor–acceptor distance ranges from 3.245 (3) to 3.421 (3) Å. The hydronium molecules play an important role in the three-dimensional network of hydrogen bonding. In fact, the H_3O^+ ion is intercalated between nitrates groups forming six bonds with nitrates groups [31]. These bonds are generated by the C_3 symmetry from two bonds: H4–O4 ••• O1=2.576 (2) and O4–H4 ••• O2=3.141 (3) Å. The first link is a strong hydrogen bond that may play an important role in the electrical conduction as well as ferroelectricity by the appearance of spontaneous polarization as a function of electric field E. The second type of link is a simple electrostatic interaction Van der Waals which ensures the stability of the crystalline structure.

4. Nonlinear studies

4.1. Second harmonic generation (SHG)

The SHG efficiency of DOTN was measured by the use of modified Kurtz and Perry technique [32,33]. In fact, in this method the crystal was finely ground into powder of known grain size of 90 μm and

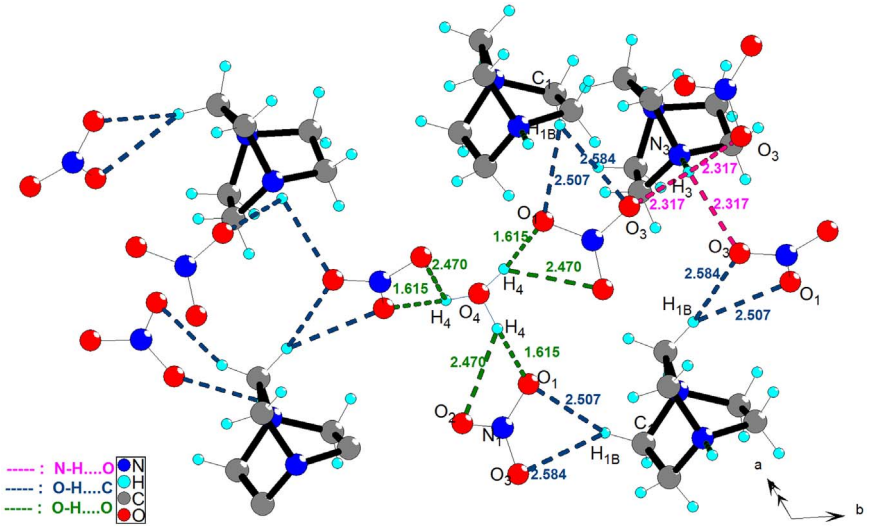

Fig. 7. Packing of the title compound illustrating the hydrogen bonding of the nitrate anion and the protonated DABCO nitrogen.

Table 4
Hydrogen-bond geometry.

D—H···*A*	*D*—H	H···*A*	*D*···*A*	*D*—H···*A*
N2—H2···O3^{iii}	0.87 (6)	2.32 (4)	2.935 (3)	128.3 (12)
N2—H2···O3^{iv}	0.87 (6)	2.32 (4)	2.935 (3)	128.3 (13)
N2—H2···O3^{v}	0.87 (6)	2.32 (4)	2.935 (3)	128.3 (12)
N3—H3···O3^{vi}	0.92 (6)	2.32 (4)	2.978 (3)	128.3 (12)
N3—H3···O3^{vii}	0.92 (6)	2.32 (4)	2.978 (3)	128.3 (12)
N3—H3···O3^{viii}	0.92 (6)	2.32 (4)	2.978 (3)	128.3 (12)
C1—H1A···O2^{iii}	0.95 (4)	2.49 (4)	3.345 (3)	150 (3)
C1—H1B···O1^{i}	0.98 (3)	2.51 (3)	3.421 (3)	156 (2)
C1—H1B···O3^{i}	0.98 (3)	2.58 (3)	3.374 (3)	138 (3)
C2—H2B···N1^{vi}	0.95 (3)	2.64 (3)	3.245 (3)	122 (3)
O4—H4···O1^{ix}	0.97 (5)	1.62 (5)	2.576 (2)	171 (5)
O4—H4···O2^{ix}	0.97 (5)	2.47 (5)	3.141 (3)	126 (4)
O4—H4···N1^{ix}	0.97 (5)	2.36 (5)	3.267 (2)	155 (4)

Symmetry codes: (iii) *y*, *x*, *z*+1/2; (iv) −*x*+1, −*x*+*y*+1, *z*+1/2; (v) *x*−*y*, −*y*+1, *z*+1/2; (vi) *y*, *x*, *z*−1/2; (vii) −*x*+1, −*x*+*y*+1, *z*−1/2; (viii) *x*−*y*, −*y*+1, *z*−1/2; (i) −*x*+*y*, −*x*+1, *z*; (ix) −*x*+*y*, −*x*, *z*.

Table 5
SHG powder intensity values for DOTN and other well-characterized materials.

Materials	I^{2w}/I^{KDP2w}	
DOTN	3.4	Under study
$[Mg_2(btc)(CH_3COO)(C_4H_9NO)_3]_n$	5	[34]
$[Cd(anp)_2Br_2{\cdot}H_2O]_n$	2.1	[35]
KDP	1	
Urea	1.8	
α-SiO_2	0.26	
$[Cd_2(4,4'\text{-bipy})_2(H_2O)_3(SO_4)_2{\cdot}3H_2O]_n$	0.27	[36]
l-Tryptophan p-nitrophenol (LTPNP)	4	[37]
Dibromo bis (L-proline) Cd (II)	2.25	[13]

powder samples were taken and densely filled between two glass slides. Powdered potassium dihydrogene phosphate of identical size 90 μm was used as a reference material as it is a well-known inorganic nonlinear optical material. A Q-switched Nd: YAG laser with 1064 nm was used as an optical source and focused on the sample. The pulse width of 8 ns and pulse rate of 10 Hz were used.

The second harmonic signal was collected in 90° geometry using

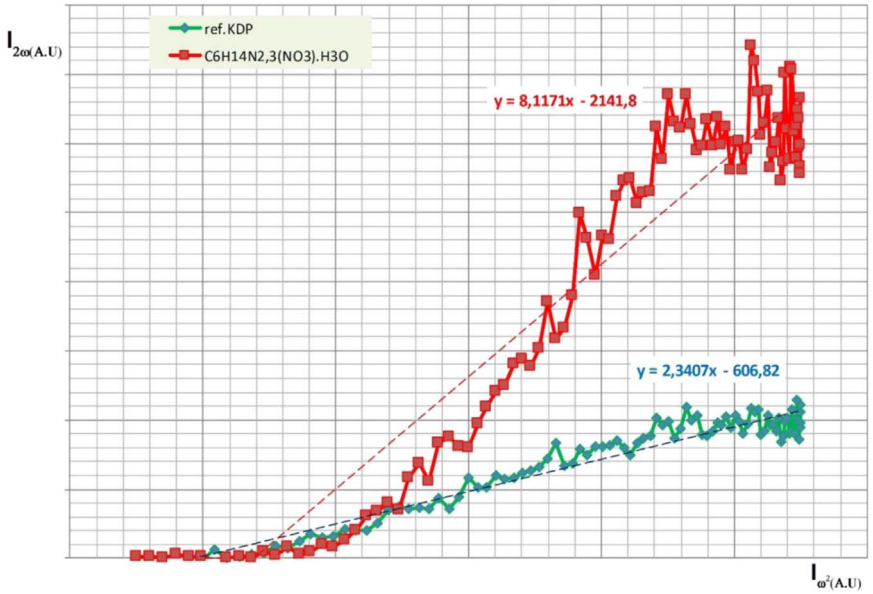

Fig. 8. Power dependence of $I_{2\omega}$ vs. I_{ω} for DOTN and KDP.

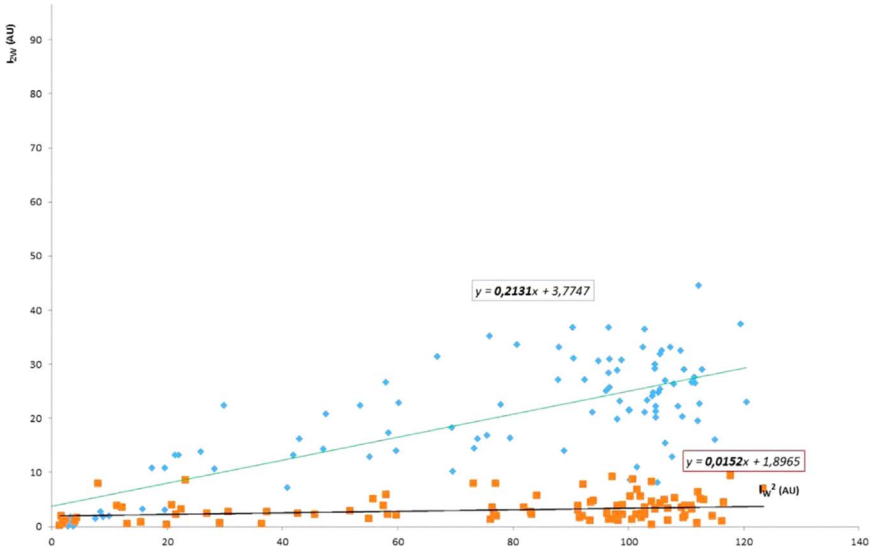

Fig. 9. Power dependence of $I_{2\omega}$ vs. I_{ω} for nitrate and water.

monochromator and photomultiplier tube setup. The SHG efficiency was 3.4 times that of standard KDP (Fig. 8). The result was compared with other non linear optical materials is shown in Table 5.

4.2. Harmonic light scattering (HLS)

The first hyperpolarizability (β) of the nitrates solved in water was measured by the second harmonic light scattering (SHLS) technique [38]. A 1064 nm fundamental wavelength of a Q-switched Nd: YAG laser was focused on the sample by a convex lens of 0.2 m in focal length. The scattered second harmonic photons ($I_{2\omega}$) were collected at a 90° geometry using a photomultiplier tube after filtering out the fundamental wave and the signal was processed in a storage oscilloscope. The first hyperpolarizability (β) of a molecule dissolved in a solvent was related to the SH scattered light intensity ($I_{2\omega}$) by:

$$\mathbf{I_{2\omega} = G(N_{Solvent}\beta^2_{Solvent} + N_{Solute}\beta^2_{Solute})I^2_{\omega}} \quad (1)$$

where $\mathbf{N_{solvent}}$ and $\mathbf{N_{solute}}$ are the values of densities of the solvent and solute molecules, respectively, G is an instrument factor, and Iω is the intensity of the incident beam.

The intensity of the second harmonic light was plotted against the incident laser light intensity to confirm the occurrence of the second-order process (Fig. 9).

The first hyperpolarizability of the sample was determined by the external solvent method [39]. From the slopes, the beta value was calculated as 1.39×10^{-30} esu by using the following formula:

$$\beta_{sample} = \sqrt{\frac{P_{solute}C_{solvent}}{P_{solvent}C_{solute}} \times \beta_{solvent}} - 1 \quad (2)$$

Interestingly, it is clearly shown that this material possesses this SHG value possibly due to the value of the first hyperpolarizability β of the nitrate because the magnitude of the SHG directly depends on the β (first hyperpolarizability) and γ (second hyperpolarizability) [40,41] at the molecular level. The delocalization of the non-bonding electrons of the oxygen atoms of the nitrate, associated with a 3 symmetry, makes it possible to obtain appreciable nonlinearity [42]. Also, may be the different mesomeric forms of nitrate forced the delocalization of the electrons without neglecting the aromatic electrons delocalization. All of these interactions play an important role in the overlapping of the wave function of the molecules.

5. Conclusion

The synthesis of this new material has been realized at room temperature by the combination of DABCO and the nitric acid. This combination has allowed us to obtain a new $C_6H_{14}N_2,(NO_3)_3{\cdot}H_3O$ phase. The FTIR spectrum analysis has significantly shown the presence of different groups such as NO_3^-, OH^- and NH^+, which confirms the protonation of the amine in the two sites. The structural determination using the X-Ray analysis of DOTN compound has established the structural model in which the asymmetric unit consists of an organic diprotonated cation $(C_6H_{14}N_2)^{2+}$, three inorganic anions and H_3O^+ molecule. These entities are linked by hydrogen bonds and π-π interactions involving a crystal structure in a three-dimensional network. The SHG efficiency of the compounds under study shows an efficiency of 3.4 times more than that of the reference crystal KDP. DOTN structure arrangement promotes an important NLO response. This can be explained by the presence of electronic delocalization along the organic-inorganic entities, without neglecting the probable impact of the nitrate ion; especially possession of a high hyperpolarizability in free state ($\beta_{(nitrate)}$=1.39×10^{-30} esu). Emphasis was put on the inorganic group of the nitrate which can induce this high hyperpolarisability. High NLO makes this hybrid compound usable in high power applications such as optoelectronic fields.

Conflicts of interest

The authors declare no competing financial interest.

Appendix A. Supporting information

Supplementary data associated with this article can be found in the online version at doi:10.1016/j.jpcs.2017.02.011.

References

[1] R.W. Munn, C.N. Ironside, Principles and Applications of Nonlinear Optical Materials, Chapman & Hall, London, 1993.
[2] Non-Linear Optical Properties of Molecules and Crystal 1–2, Academic Press, New York, 1987.
[3] Mark J. Gunning, Roger E. Raab, W.łodimierz Kucharczyk, J. Opt. Soc. Am. B 18 (2001) 1092–1098.
[4] I. Ledoux, J. Zyss, J.S. Siegel, L.J. Brienne, J.M. Lehn, J. Chem. Phys. Lett. (1990)) 172.
[5] X. Ren, D. Xu, D. Xue, J. Cryst. Growth 310 (2008) 2005–2009.
[6] N. Ennaceur, I. Ledoux-Rak, A. Singh, T. Mhiri, K. Jarraya, J. Phys. B 428 (2013) 106–109.

[7] N. Ennaceur, I. Ledoux-Rak, T. Mhiri, J. Phys. B 410 (2013) 182–187.
[8] P. Vijayakumar, G. Anandha Babu, P. Ramasamy, J. Mater. Res. Bull. 47 (2012) 957–962.
[9] L.R. Mingabudinova, V.V. Vinogradov, V.A. Milichko, E. Hey-Hawkins, A.V. Vinogradov, J. Chem. Soc. Rev. 45 (2016) 5408.
[10] T. Jayanalina, G. Rajarajan, K. Boopathi, K. Sreevani, J. Cryst. Growth 426 (2015) 9–14.
[11] K. Boopathi, P. Rajesh, P. Ramasamy, J. Mater. Res. Bull. 47 (2012) 2299–2305.
[12] A. Bhaskaran, S. Arjunan, C.M. Raghavan a, R. MohanKumar c, R. Jayavel, J. Cryst. Growth 310 (2008) 4549–4553.
[13] K. Boopathi, P. Ramasamy, J. Mol. Struct. 1080 (2015) 37–43.
[14] Manoj K. Gupta, Nidhi Sinha, Binay Kumar, J. Phys. B 406 (2011) 63–67.
[15] K. Selvaraju, K. Kirubavathi, J. Spectrochim. Acta Part A: Mol. Biomol. Spectrosc. 115 (2013) 537–543.
[16] Y. Le Fur, M. Bagieu-Beucher, R. Masse, J.F. Nicoud, J.P. Levy, J. Chem. Mater. 8 (1996) 68–75.
[17] M. Meiyappan, M. Bagieu-Beucher, Y. Le Fur, J. Z. Kristallog. NCS 214 (1999) 201–202.
[18] A. Praveen Menezes, A. Jayarama, J. Mol. Struct. 1075 (2014) 246–253.
[19] S. Vodnalaa, A.K.D. Bhavania, R. Kamutama, V.G.M. Naidub, Promilac, Ch Prabhakarc, J. Bioorg. Med. Chem. Lett. 26 (I 16) (2016) 3973–3977.
[20] Q. Jia, L. Chen, G. Yang, J. Wang, J. Wei, Z. Du, J. Tetrahedron Lett. 56 (52) (2015) 7150–7153.
[21] X. Han, P. Hu, Ch Shi, W. Zhang, J. Mol. Struct. 1127 (2017) 372–376.
[22] W. Zhang, H.-Y. Ye, H.-L. Cai, J.-Z. Ge, R.-G. Xiong, S.P.D. Huang, J. Am. Chem. Soc. 132 (2010) 7300–7302.
[23] Y. Zhang, W. Zhang, S.-H. Li, Q. Ye, H.-L. Cai, F. Deng, R.-G. Xiong, S.P.D. Huang, J. Am. Chem. Soc. 134 (2012) 11044–11049.
[24] Z.-H. Sun, X.-Q. Wang, J.-H. Luo, S.-Q. Zhang, D.-Q. Yuan, M.-C. Hong, J. Mater. Chem. C1 (2013) 2561–2567.
[25] L. Catalano, S. Perez-Estrada, G. Terraneo, T. Pilati, G. Resnati, P. Metrangolo, M.A. Garcia-Garibay, J. Of. Am. Chem. Soc. 137 (2015) 15386–15389.
[26] G.M. Sheldrick, J. Acta Cryst. A71 (2015) 3–8.
[27] G.M. Sheldrick, J. Acta Cryst. A64 (2015) 112–122.
[28] N. Sudharsana, V. Krishnakumar, R. Nagalakshmi, J. Cryst. Growth 398 (2014) 45–57.
[29] S. Stella Marya, S. Shahil Kirupavathyb, R. Gopalakrishnan, J. Opt. 125 (2014) 3837–3843.
[30] K.E. Knope, C.L. Cahill, J. Acta Crystallogr. E63 (2007) 2955.
[31] K. Bouchouit, Z. Sofiani, B. Derkowska, S. Abed, N. Benali-cherif, M. Bakasse, B. Sahraoui, J. Opt. Commun. 278–1 (2007) 180–186.
[32] S.K. Kurtz, T.T. Perry, J. Appl. Phys. 39 (1968) 3798–3813.
[33] N. Ennaceur, K. Jarraya, A. Singh, I. Ledoux-Rak, T. Mhiri, J. Phys. Chem. Solids 73 (2012) 418–422.
[34] S. Ma, J.A. Fillinger, M.W. Ambrogio, J.-L. Zuo, H.-C. Zhou, J. Inorg. Chem. Commun. 10 (2007) 220–222.
[35] W.-W. Zhou, W. Zhao, B. Wei, F.-W. Wang, Y.-H. Chen, W.-Y. Fang, X. Zhao, J. Inorg. Chim. Acta 386 (2012) 17–21.
[36] Y. Zhao, L. Luo, C. Liu, M. Chen, W.-Y. Sun, J. Inorg. Chem. Commun. 14 (2011) 1145–1148.
[37] R. Omegala Priakumari, S. Grace Sahaya Sheba, M. Gunasekaran, J. Opt. 125 (2014) 4633–4636.
[38] Giordmaine, J. Phys. Rev. Lett. 138 (1965) 1599.
[39] M.A. Pauley, H.W. Guan, C.H. Wang, A.K.Y. Jen, J. Chem. Phys. 104 (1996) 7821–7829.
[40] H. Yadav, N. Sinha, B. Kumar, J. Mater. Res. Bull. 64 (2015) 194–199.
[41] C.W. Dirk, R.J. Twieg, G. Wagniere, J. Am. Chem. Soc. 108 (1986) 5387–5395.
[42] H.S. Nalwa, S. Miyata, Nonlinear Optics of Organic Molecules and Polymers, CRC, Boca Raton, FL, 1997.